

# PID CONTROLLER DESIGN FOR DC MOTOR POSITION ANALYSIS AND APPLICATION TO ANKLE REHABILITATION SYSTEM

M.A.R. Azizi<sup>1</sup>, K. Osman<sup>1</sup>, A. Jaafar<sup>1</sup> and K. Suzumori<sup>2</sup>

<sup>1</sup>Faculty of Electronic and Computer Engineering,  
Universiti Teknikal Malaysia Melaka, Hang Tuah Jaya, 76100 Durian  
Tunggal, Melaka, Malaysia.

<sup>2</sup>School of Engineering,  
Tokyo Institute of Technology, Meguro City,  
152-8550 Tokyo, Japan.

Corresponding Author's Email: [khairuddin.osman@utem.edu.my](mailto:khairuddin.osman@utem.edu.my)

**Article History:** Received 1 June 2021; Revised 5 September 2021;  
Accepted 29 December 2021

**ABSTRACT:** Sprain ankle rehabilitation is a therapeutic exercise to recover ankle strength and maintain the muscles. Recently, Direct Current (DC) motors are widely used in rehabilitation exercise applications as the mechanism's joint of a system. The DC motors allow the desired maximum and minimum range of motion during the therapist exercise. However, the control system is not stable enough for the position response of the DC motor. The objective of this study is to the purpose of the modeling control of DC motor using the Proportional-Integral-Derivative (PID) controller algorithm. The control system algorithm has been realized with implementation of PID controller for more efficient speed and position control. The PID controller is applied to analyze the performance using MATLAB software. The proposed results are compared to the performance of the system between with or without the PID controller. Based on the result obtained, the modelling controller design increased the rising time with 60.54%, settling time with 65.43% and maintained the steady-state error with zero overshoot percentage. This system using DC motor with PID controller tune is expected to improvise the motorized rehabilitation device for the immersed system technology of the robotic revolution.

**KEYWORDS:** *Ankle Rehabilitation; DC Motor; PID Controller; Position Control; MATLAB Simulink*

## 1.0 INTRODUCTION

A sprained ankle is musculoskeletal joint pain and disability because of overexertion movement direction commonly occurs for the lower limb musculoskeletal injury [1-2]. These ligament injuries can cause improper or excessive movement within the joint due to external factors. Several studies have revealed that ankle sprain injuries can happen to active individuals especially athletes because of actively used muscle and musculoskeletal joint work [3-4]. Previous studies as reported in [5-6] highlighted that conduct the warm-up or stretching as routine activities able to increase muscle extensibility, stimulate blood flow to the periphery, tendon suppleness and enhance free coordinated movement. Figure 1 depicts the model of an ankle-foot structure where the majority of people affected by the ankle ligament stretch suffered [7-8]. According to the work in [9], the injury will occur the anterior talofibular or tibiofibular ligament in the early stage then followed by calcaneofibular ligament injury.

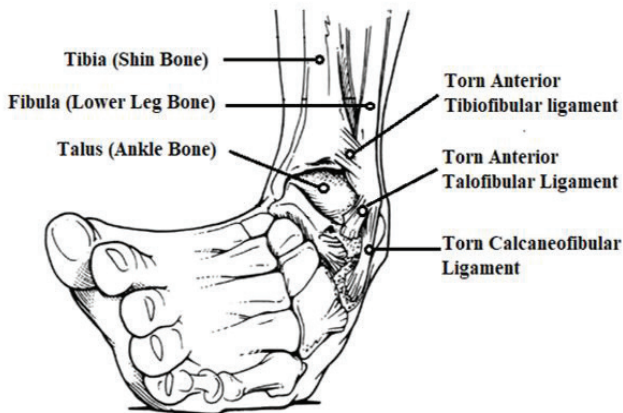


Figure 1: The model of an ankle-foot and ligament stretch structure [8]

A study by [10] mentioned that normally the ligament needs six weeks to heal but depends on the ankle sprain level of everyone. As noted in [11], the immobilization will improve faster recovery compared to therapeutic exercise to regain full function strength of the ankle joint.

The rehabilitation technique is divided into manual rehabilitation therapists and robotic rehabilitation therapists. The manual rehabilitation therapist approach uses simple devices available in clinics or any physiotherapist outlets such as elastic band, roller foams and wobble boards. The elastic band is made of multi-shape strips with resistive elastic used for muscular strengthening. Roller foams and wobble boards are used to improve balance and proprioception.

However, the study in [12] stressed that these low complexity devices only allow simple rehabilitation exercise only with the patient's effort strength and does not have specific limitation guidance for angle range to avoid re-injury. Furthermore, this primitive passive device not able to perform any data acquisition of a patient's exercise.

Currently, the robotic system technology has immersed with huge mechatronic devices that need to concern the mechanical design, actuator for the joint structure, control system and safety [13]. This innovation was able to help assist routine work with more precise and reduce the need for human manpower in the future. Safety is the most important risk need to concern because related to human during therapist to secure patients from harm or unintentional injury. With the reference to [14-15], the robotic system has assisted operation devices in terms of functional activity exercise instruction, real-time feedback monitoring and sensor to read the accuracy of angle rotation.

In this paper, the actuator selected only focused on the DC motor as the actuator because a recent rehabilitation exercise system is driven by the motor actuator growing in the field of mechatronics. There are many advantages of DC motor compared to other actuators available but still depends on the system requirements. DC motor is widely preferred in industries because of high-performance systems requiring minimum torque ripple, speed response, rapid dynamic torque, good inertia and high efficiency. Furthermore, the DC motor has required position feedback and speed control with high controllability. It also has the best performance with long-term productivity investment [16]. In comparison to pneumatic, it much more expensive and complicated to set up the equipment system because need an extra component which is an air compressor with some acoustic noises. Pneumatic also has low force and speed to drive the rehabilitation system. But most of the pneumatic device is suitable for active orthotics because similar to the human muscle concept. Another actuator is hydraulic that usually used in heavy orthoses/exoskeletons to provide high power. However, the fact that hydraulic components are heavy and the hardware design must support this component weight [17]. The DC motor is smaller in size and has no vibrate but still can give the same torque.

The objectives of the study are the purpose of the modelling control of DC motor using the Proportional-Integral-Derivative (PID) controller. The PID controller is applied to analyze and improve the performance in terms of settling time, rise time and overshoot percentage of DC motor position and speed.

The paper is organized as follows: Section 2.0 introduces the operating principle, calculation of the mathematical model of DC motor with important parameters such as the electrical and mechanical times constant therefore, the friction can be estimated. Section 3.0 concentrates on the experimental result and discussion based on the analysis. Section 4.0 describes the conclusions and future recommendations.

## 2.0 METHODOLOGY

This section describes the process of modeling a DC motor to analyze the performance of the system using the PID controller to increase the performance in terms of settling time, rise time and overshoot percentage. Figure 2 shows the sequence of PID Controller Implementation on the DC Motor. The mathematical model of the DC motor is calculated then implements the transfer function based on the parameter specification of motor. Next is getting the initial reading value of the motor position without the PID controller. Then  $K_p$ ,  $K_i$  and  $K_d$  are applied with a closed-loop system for the position and speed of the actuator. Lastly, the feedback of all results from the comparison and analyze the output in terms of rise time, settling time and overshoot percentage.

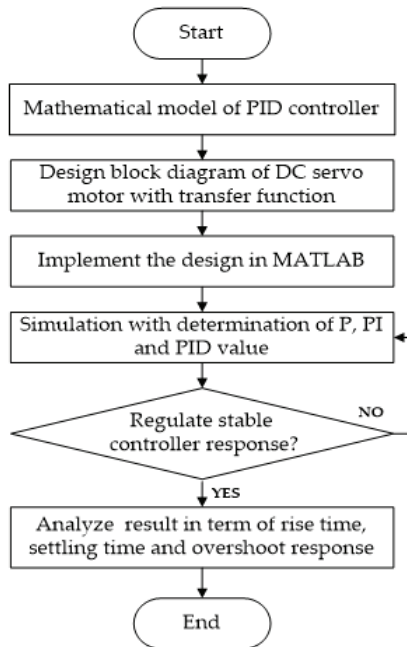


Figure 2: Sequence of PID controller implementation on the DC motor

## 2.1 Modelling of DC Motor

A DC motor is divided into two main components which are an electrical component and a mechanical component. Figure 3 shows the schematic equivalent circuit of an armature controlled DC motor with a fixed field circuit.

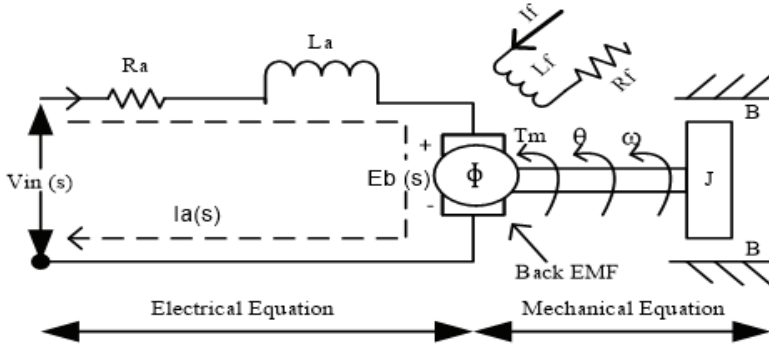


Figure 3: Equivalent circuit of an armature-controlled DC motor

Equation (1) shows the DC motor equivalent model with Kirchoff Voltage Law. The circuit will transform into s domain using Laplace transform such as

$$Vin(s) = Ia(s)Ra + Ia(s)LaS + Eb(s) \quad (1)$$

While the armature current is denoted by the following equation:

$$Is(s) = \left[ \frac{1}{[LaS + Ra]} \right] (Vin(s) - Eb(s)) \quad (2)$$

When the input voltage ( $V_{in}$ ) is supplied, the armature current ( $I_a$ ) went through the resistance ( $R_a$ ) and the inductance ( $L_a$ ) produced the magnetic flux ( $\phi$ ). The motor torque ( $T_m(s)$ ) is proportional to the product of the armature current and the air gap flux. When  $K_t$  is a torque constant, the motor torque yielded as

$$Tm(s) = Kt.Ia(s) \quad (3)$$

Equation (4) shows the armature current credits the torque which is applied to the equivalent momentum of inertia ( $J$ ) and the equivalent coefficient of friction ( $B$ ) such as

$$T = J \frac{d^2\theta}{dt^2} + B \frac{d\theta}{dt} \tag{4}$$

The angular velocity after converting into Laplace Transform depicted as

$$\omega(s) = \frac{1}{[Js + B]} (Tm(s)) \tag{5}$$

The back electromotive force (Eb(s)) is proportional to an angular velocity where

$$Eb(s) = Kb.\omega(s) \tag{6}$$

The angular displacement denotes as

$$\theta(s) = \frac{1}{s} \omega(s) \tag{7}$$

Therefore, the transfer function of the armature DC motor is obtained from the input voltage, Vin(s) to the output angle, θ(s) where

$$\frac{\theta(s)}{Vin(s)} = \frac{Kt(s)}{s[(Las + Ra)(Js + B) + (KtKb)]} \tag{8}$$

Figure 4 shows the block diagrams consist of the above equations. The input ports are stated as the input voltage using the step response while the output ports are the angular speed (ω) and position (θ).

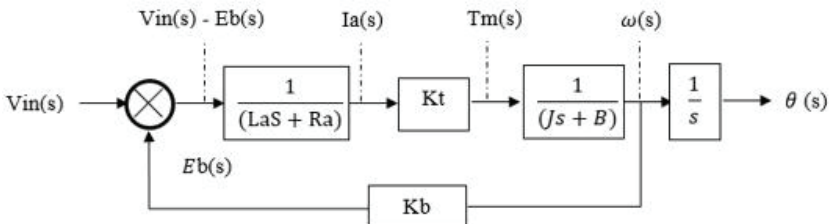


Figure 4: Block diagram of the DC motor position and angular speed

## 2.2 Simulator of PID Controller

PID control can perform a good control which can be set externally therefore, it is widely used in the electronic industries. Figure 5 shows the block diagram of the PID controller. Each of the three components of P, I and D have different functionality and it covers one the controller task such as:

- i. P is a proportional sensitivity,  $K_p$ .
- ii. I is an integral action time,  $T_n$ .
- iii. D is a derivative action time,  $T_v$ .

Table 1: Manual tuning of PID parameter independently

Parameter	Steady-State Error (SSE)	Overshoot (OS)	Settling time, $t_s$	Rising time, $t_r$	Stability
$K_p$	Decrease	Increase	Small change	Decrease	Degrade
$K_i$	Eliminate	Increase	Increase	Decrease	Degrade
$K_d$	Theoretically no effect	Decrease	Decrease	Minor Change	Improve if $K_d$ is small enough

Table 1 shows the manual tuning of the PID parameter independently. To increase the settling time, ( $t_s$ ) before the final value reaching its Steady State Error (SSE), the  $K_i$  needs to increase as  $K_p$  should be in small changes and  $K_d$  decreases its values. To obtain the lowest overshoot percentage (OS), the  $K_p$  have to increase until the output oscillates into reaching stability and shorten the settling time ( $t_s$ ). However, some of the systems cannot accept the slow rising time, thus decreasing the values of  $K_p$  and  $K_i$ , as well as the changing of  $K_d$  can fasten the rising time ( $t_r$ ). Degrading the values of  $K_p$  and  $K_i$  can improve the stability and where  $K_d$  is in small changes. Finally, decreasing of  $K_p$  value and eliminating  $K_i$  with no changing value on  $K_d$  can meet the steady-state error (SSE) equals to 1. The following equation is linked to Figure 5 where

$$u(t) = K_p e(t) + \frac{1}{T_i} \int_0^t e(t) dt + T \frac{de(t)}{dt} \quad (9)$$

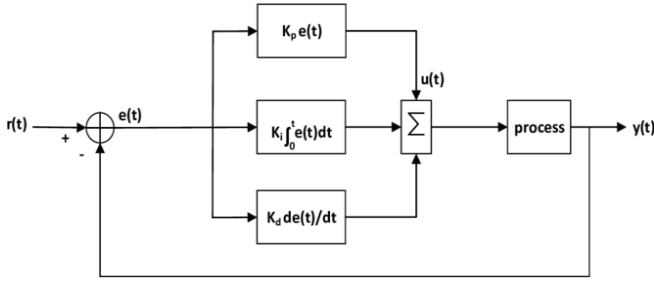


Figure 5: PID controller block diagram

Equation (10) shows  $K_i$  and  $K_d$  are substituted by  $T_i$  and  $T_d$  represents an integration of the time and derivative time, respectively. The advantage of  $T_i$  and  $T_d$  is based on the physical meaning.

$$u(t) = K_p e(t) + \frac{1}{T_i} \int_0^t e(t) dt + T_d \frac{de(t)}{dt} \quad (10)$$

Figure 6 shows the completion of DC motor modelling using MATLAB 2020 Simulink. The parameters were set in accordance to the specification of the DC motor for example, using the datasheets. The calculation is made based on the specification produced by the parameters as shown in Table 2.

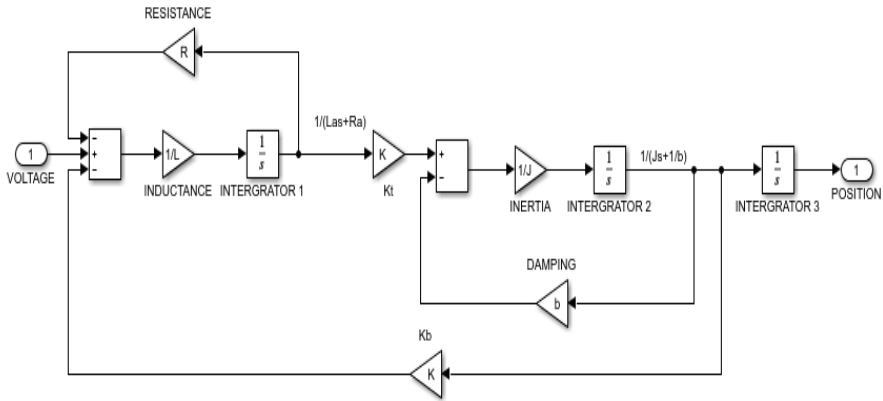


Figure 6: DC motor modeling using MATLAB Simulink



Table 2: Parameter of DC servo motor

No	Parameter	Abbreviation	Value	Units
1	Rated Voltage	Vin	12	V
2	Armature Resistance	Ra	1	$\Omega$
3	Armature Inductance	La	0.23	mH
4	Applied Voltage	Eb	4-6	V
5	Motor Torque	T	1.02	N.m
6	Moment of Inertia	J	0.02	$\text{Kg.m}^2$
7	Viscous Friction	B	0.03	Nms/rad
8	Torque Constant	Kt	0.021	Nm/A
9	Electromotive Force Constant	Kb	0.021	Vs/rad

### 3.0 RESULTS AND DISCUSSION

In this section, the parameter from the PID controller is used as a result to eliminate all errors and getting the absolute performance when the DC motor turned to its position in each angle trajectory. Figure 6 shows the simulation result of the open-loop based on the DC motor modeling using MATLAB Simulink and Equation (8). Next, the PID controller is placed on the configuration of MATLAB Simulink model with the combination of DC Motor modelling as depicted in Figure 7.

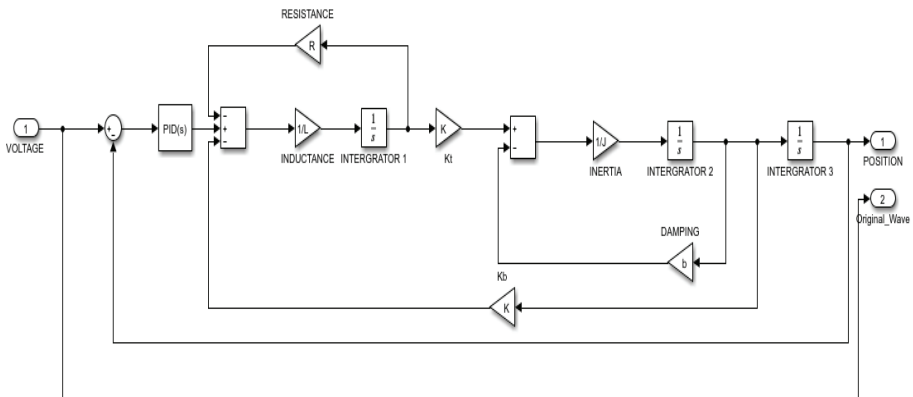


Figure 7: PID controller combine with DC motor modelling

At the beginning process, the PID auto-tuning is used to estimate the nearest value of  $K_p$ ,  $K_i$  and  $K_d$  parameters from the experiment in real-time. The PID auto-tuning estimated the nearest values with  $K_p = 2.56$ ,  $K_i = 1.40$  and  $K_d = 0.00017$ . However, the values still can be improved to get a better output response. The test for each parameter starts from P-ID, PI-D and PID to get the suitable absolute value for this modeling system. A better output response can be yielded when increasing the parameters in Table 1. Figure 8 shows the result of  $K_p = 1.80$ ,  $K_i = 1.15$

and  $K_d = 0.00018$  and by comparing with the result without PID controller, the PID controller result is more stable with the rising time is 0.014, the settling time is 0.0234 and the overshoot percentage is 0.0736%.

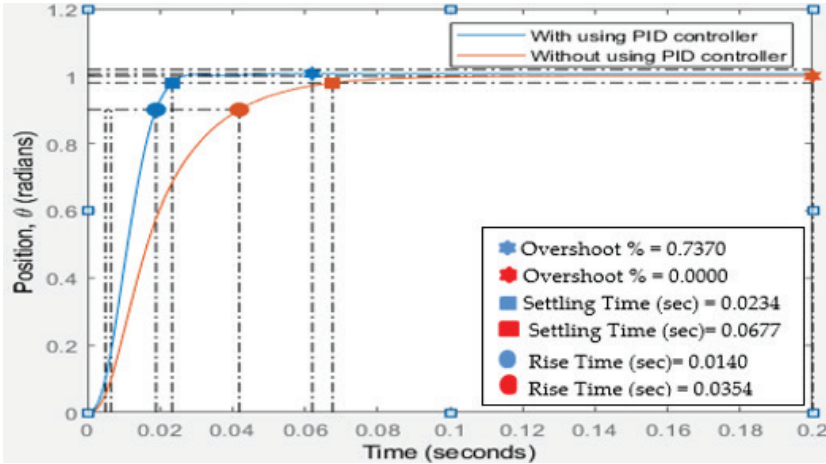


Figure 8: The difference in a DC motor system with and without PID controller

#### 4.0 CONCLUSION

In this paper, a DC motor control system is introduced for position control simulated using MATLAB/Simulink tool. The result of each controller is discussed and analyzed in terms of the performance criteria. The implementation of the PID controller has a more efficient and accurate output angle of DC motor position in terms of rising time, settling time and overshoot percentage. According to the result obtained, a closed-loop system is better than an open-loop system in order to reach the target position angle value. Furthermore, the modeling controller design increased the rising time to 60.54%, the settling time to 65.43% and maintained the steady-state value with zero overshoot percentage. The DC motor with a PID controller will be suggested for future study in the ankle rehabilitation program for example, the patients with the real ankle sprain injury. The system is also suggested to embed with a gyro sensor and gimbal method for more precise angular feedback.

## ACKNOWLEDGMENTS

The authors would like to acknowledge the Faculty of Electronics and Computer Engineering and Universiti Teknikal Malaysia Melaka for all facilities and the research grant, PJP/2019/FKEKK-CETRI/CRG/S01701.

## REFERENCES

- [1] E. Delahunt, C. M. Bleakley, D. S. Bossard, B. M. Caulfield, C. L. Docherty, C. Doherty, F. Fourchet, D. T. Fong, J. Hertel, C. E. Hiller, and T. W. Kaminski, "Clinical Assessment of Acute Lateral Ankle Sprain Injuries (ROAST): 2019 Consensus Statement and Recommendations of the International Ankle Consortium", *British Journal of Sports Medicine*, vol. 52, no. 20, pp. 1304–1310, 2018.
- [2] R. A. Hauser, E. E. Dolan, H. J. Phillips, A. C. Newlin, R. E. Moore, and B. A. Woldin, "Ligament Injury and Healing: A Review of Current Clinical Diagnostics and Therapeutics", *The Open Rehabilitation Journal*, vol. 6, no. 1, pp. 1–20, 2013.
- [3] L. Chinn and J. Hertel, "Rehabilitation of Ankle and Foot Injuries in Athletes", *Clinics in Sports Medicine*, vol. 29, no. 1, pp. 157–167, 2010.
- [4] J. J. Fraser, J. M. Hart, S. F. Saliba, J. S. Park, M. Tumperi, and J. Hertel, "Multisegmented Ankle-Foot Kinematics during Gait Initiation in Ankle Sprains and Chronic Ankle Instability", *Clinical Biomechanics*, vol. 68, pp. 80–88, 2019.
- [5] A. J. Fradkin, T. R. Zazryn, and J. M. Smoliga, "Effects of Warming-Up on Physical Performance: A Systematic Review with Meta-Analysis", *The Journal of Strength & Conditioning Research*, vol. 24, no. 1, pp. 140–148, 2010.
- [6] M. P. Mchugh and C. H. Cosgrave, "To Stretch or Not to Stretch : The role of Stretching in Injury Prevention and Performance", *Scandinavian Journal of Medicine & Science in Sports*, vol. 20, no. 2, pp. 169–181, 2010.
- [7] Y. H. Tsoi and S. Q. Xie, "Impedance Control of Ankle Rehabilitation Robot", in *International Conference on Robotics and Biomimetics*, Bangkok, Thailand, 2008, pp. 840-845.
- [8] M. A. R. Azizi, A. Jaafar, and K. Osman, "Performance Analysis for Sprain Ankle Rehabilitation System using Gyro Sensor", *International Journal of Advanced Science and Technology*, vol. 29, no. 6s, pp. 860–872, 2020.
- [9] H. Chaudhry, N. Simunovic, and B. Petrisor, "Cochrane in CORR ®: Surgical versus Conservative Treatment for Acute Injuries of the Lateral Ligament Complex of the Ankle in Adults", *Clinical Orthopaedics and Related Research®*, vol. 473, no. 1, pp. 17–22, 2015.

- [10] P. A. Gribble, C. M. Bleakley, B. M. Caulfield, C. L. Docherty, F. Fourchet, D. T. P. Fong, J. Hertel, C. E. Hiller, T. W. Kaminski, P. O. McKeon, and K. M. Refshauge, "Evidence Review for the 2016 International Ankle Consortium Consensus Statement on the Prevalence, Impact and Long-Term Consequences of Lateral Ankle Sprains", *British Journal of Sports Medicine*, vol. 50, no. 24, pp. 1496–1505, 2016.
- [11] S. Guillo, T. Bauer, J. W. Lee, M. Takao, S. W. Kong, J. W. Stone, P. G. Mangone, A. Molloy, A. Perera, C. J. Pearce, and F. Michels, "Consensus in Chronic Ankle Instability: Aetiology, Assessment, Surgical Indications and Place for Arthroscopy", *Orthopaedics & Traumatology: Surgery & Research*, vol. 99, no. 8, pp. S411–S419, 2013.
- [12] J. Yoon, J. Ryu and K. B. Lim, "Reconfigurable ankle Rehabilitation Robot for Various Exercises", *Journal of Robotic Systems*, vol. 22, no. S1, pp. S15–S33, 2006.
- [13] E. Garcia, M. A. Jimenez, P. G. De Santos, and M. Armada, "The Evolution of Robotics Research", *IEEE Robotics & Automation Magazine*, vol. 14, no. 1, pp. 90–103, 2007.
- [14] H. I. Krebs, J. J. Palazzolo, L. Dipietro, M. Ferraro, J. Krol, K. Ranekleiv, B. T. Volpe, and N. Hogan, "Rehabilitation Robotics: Performance-Based Progressive Robot-Assisted Therapy", *Autonomous Robots*, vol. 15, no. 1, pp. 7–20, 2003.
- [15] M. Zhang, T. C. Davies, and S. Xie, "Effectiveness of Robot-Assisted Therapy on Ankle Rehabilitation—A Systematic Review", *Journal of Neuroengineering and Rehabilitation*, vol. 10, no. 1, pp. 1–16, 2013.
- [16] S. M. Hatem, G. Saussez, M. Della Faille, V. Prist, X. Zhang, D. Dispa, and Y. Bleyenheuft, "Rehabilitation of Motor Function After Stroke: A Multiple Systematic Review Focused on Techniques to Stimulate Upper Extremity Recovery", *Frontiers in Human Neuroscience*, vol. 10, pp. 1–22, 2016.
- [17] A. Petcu, M. Georgescu, and D. Tarniță, "Actuation Systems of Active Orthoses used for Gait Rehabilitation", *Applied Mechanics and Material*, vol. 880, pp. 118–123, 2018.